SUPPORTING INFORMATION

Experimental Evidence of a Diatropic Ring Current Occurring in the Metal Cluster $[\{(C_5Me_4H)_2La\}_3Sn_2Bi_3]^{2-}$

Yannick R. Lohse,[1‡] Julia Rienmüller,[1‡] Bastian Weinert,[1] Neeshma Mathew,[2‡] Jörn Schmedt auf der Günne,[2*] Florian Weigend,[3*] Yannick J. Franzke,[3*] and Stefanie Dehnen[1*]

[1] Karlsruhe Institute of Technology, Institute of Nanotechnology, Herrmann-von-Helmholtz-Platz 1, 76344 Eggenstein-Leopoldshafen, Germany. Email: stefanie.dehnen@kit.edu.

[2] University of Siegen, Faculty IV: School of Science and Technology, Department of Chemistry and Biology, Inorganic Materials Chemistry and Center of Micro- and Nanochemistry and Engineering (Cμ), Adolf-Reichwein-Straße 2, 57068 Siegen, Germany, Email: gunnej@chemie.uni-siegen.de.

[3] Philipps-Universität Marburg, Fachbereich Chemie, Hans-Meerwein-Straße 4, 35043 Marburg, Germany, Email: yannick.franzke@chemie.uni-marburg.de, florian.weigend@chemie.uni-marburg.de.

[‡] These authors contributed equally.

Contents:

1. Light-Microscopic Images of the Single Crystals

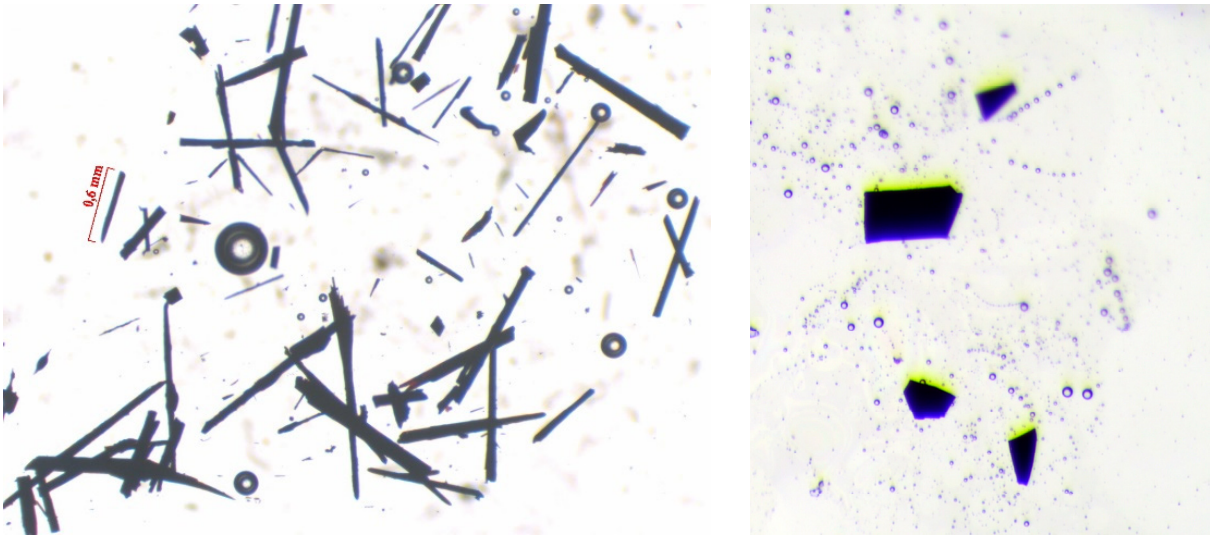

Supplementary Figure 1 | Crystal photographs of compounds [K(crypt-222)]$_2$[1]·0.66(C_6H_5Me) and [K(crypt-222)]$_2$[2]·0.25($C_5Me_4H_2$)·0.25*n*-hexane taken through a light microscope.

2. Single Crystal X-ray Diffraction (SCXRD) Data

Supplementary Table 1 | Crystallographic data and refinement parameters for compound $[K(crypt\text{-}222)]_2[1]\cdot 0.66(C_6H_5Me)$.

Chemical formula	$[K(crypt\text{-}222)]_2\{(C_5Me_4H)_2La\}_3Sn_2Bi_3]\cdot 0.66(C_6H_5Me)$
Formula weight/ g·mol^{-1}	2900.81
Empirical formula	$C_{92.67}H_{155.33}K_2N_4O_{12}Sn_2Bi_3La_3$
Empirical formula weight	2900.81
Temperature/K	100
crystal color, shape	black needle
Crystal system	monoclinic
Space group	$P2_1/n$
a/Å	15.9933(7)
b/Å	28.0507(12)
c/Å	27.0409(11)
α/°	90
β/°	90.246(3)
γ/°	90
Volume/Å^3	12131.1(9)
Z	4
ρ_{calc}/g·cm^{-3}	1.588
μ/mm^{-1}	5.888
F(000)	5621
Crystal size/mm^3	0.01 × 0.01 × 0.6
Radiation	MoKα (λ = 0.71073·10^{-10} m)
2Θ range for data collection/°	2.904 to 53.576
Index ranges	$-20 \le h \le 20$, $-35 \le k \le 35$, $-33 \le l \le 34$
Absorption correction type	spherical
Reflections collected	140291
Independent reflections	25642 [R_{int} = 0.1118, R_{sigma} = 0.0991]
Data/restraints/parameters	25642/319/1196
Goodness-of-fit on F^2	0.897
Final R indexes [$I \ge 2\sigma(I)$]	R_1 = 0.0454, wR_2 = 0.0963
Final R indexes [all data]	R_1 = 0.1011, wR_2 = 0.1097
Largest diff. peak/hole/e·Å^{-3}	1.197/–0.680
CCDC number	2287306

Supplementary Table 2 | Crystallographic data and refinement parameters for compound $[K(crypt\text{-}222)]_2[2]\cdot 0.25(C_5Me_4H_2)\cdot 0.25n$-hexane.

Chemical formula	$[K(crypt\text{-}222)]_2\{((C_5Me_4H)_2Ce\}_3TlBi_4]\cdot 0.25(C_5Me_4H_2)\cdot 0.25n$-hexane
Formula weight/ g·mol^{-1}	3060.30
Empirical formula	$C_{93}H_{155.25}K_2N_4O_{12}TlBi_4Ce_3$
Empirical formula weight	3060.30
Temperature/K	100
Crystal color, shape	black block
Crystal system	monoclinic
Space group	$P2_1/n$
a/Å	15.954(4)
b/Å	28.0512(19)
c/Å	26.982(3)
α/°	90
β/°	90.462(9)
γ/°	90
Volume/Å^3	12074(3)
Z	4
ρ_{calc}/g·cm^{-3}	1.683
μ/mm^{-1}	8.359
F(000)	5849
Crystal size/mm^3	0.3 × 0.6 × 0.5
Radiation	MoKα (λ = 0.71073·10^{-10} m)
2Θ range for data collection/°	4.144 to 50.0
Index ranges	–18 ≤ h ≤ 18, –33 ≤ k ≤ 33, –32 ≤ l ≤ 32
Absorption correction type	multi-scan
Reflections collected	220601
Independent reflections	21239 [R_{int} = 0.1458, R_{sigma} = 0.0666]
Data/restraints/parameters	21239/12/1140
Goodness-of-fit on F^2	1.092
Final R indexes [$I \geq 2\sigma(I)$]	R_1 = 0.0572, wR_2 = 0.1184
Final R indexes [all data]	R_1 = 0.0901, wR_2 = 0.1272
Largest diff. peak/hole/e·Å^{-3}	1.602/–0.987
CCDC number	2287307

3. Supplementary Crystallographic Figures of Compounds [K(crypt-222)]$_2$[1]·0.66(C_6H_5Me) and [K(crypt-222)]$_2$[2]·0.25($C_5Me_4H_2$)·0.25*n*-hexane

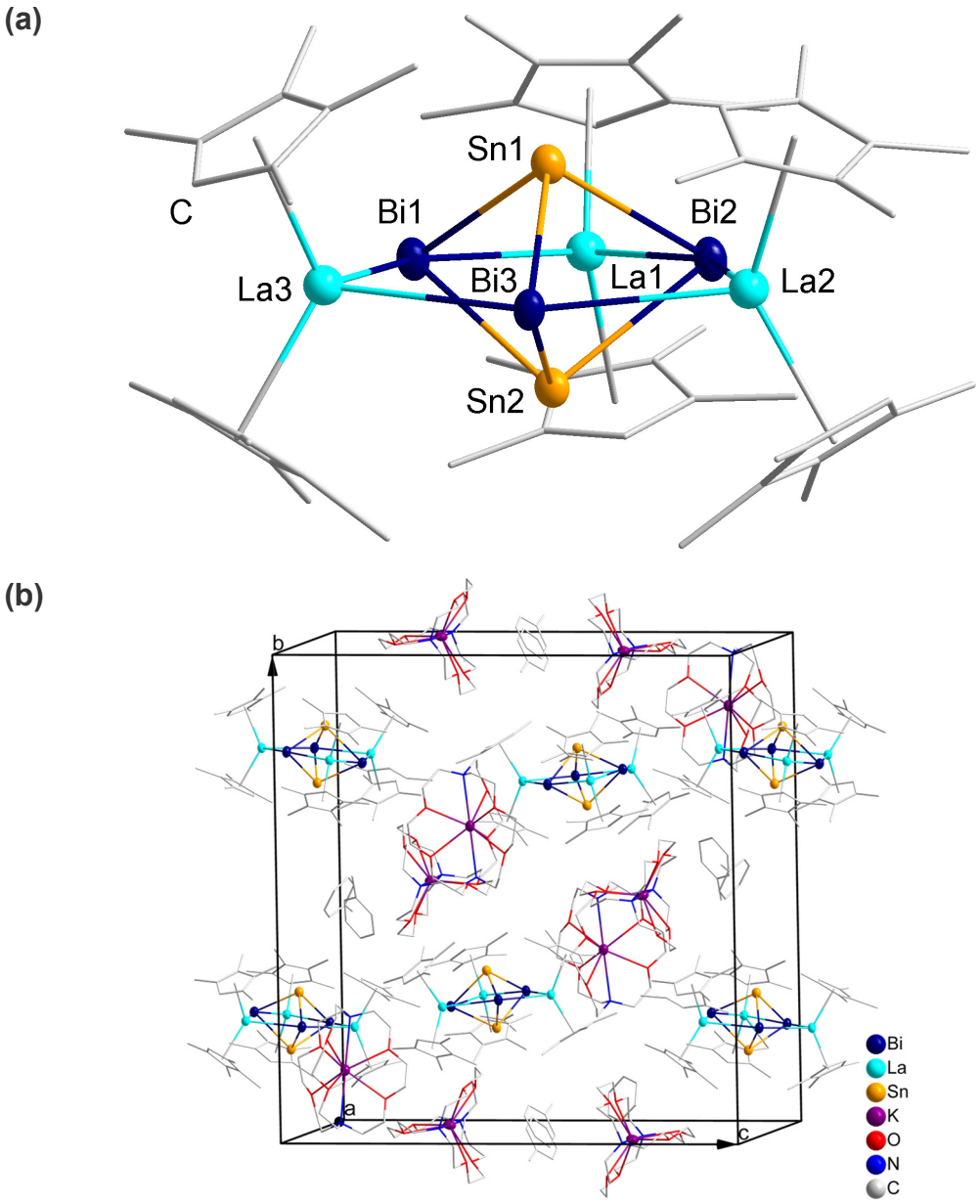

Supplementary Figure 2 | Crystal structure of [K(crypt-222)]$_2$[1]·0.66(C_6H_5Me). a, Side view of the anion $[\mathbf{1}]^{2-}$ with atom labelling scheme of the heavy atoms. **b,** view of the unit cell of [K(crypt-222)]$_2$[**1**]·0.66(C_6H_5Me). H atoms are omitted for clarity. All non-hydrogen atoms except for those of the free C_6H_5Me molecules were refined using anisotropic displacement parameters. All hydrogen atoms were refined by using a riding model.

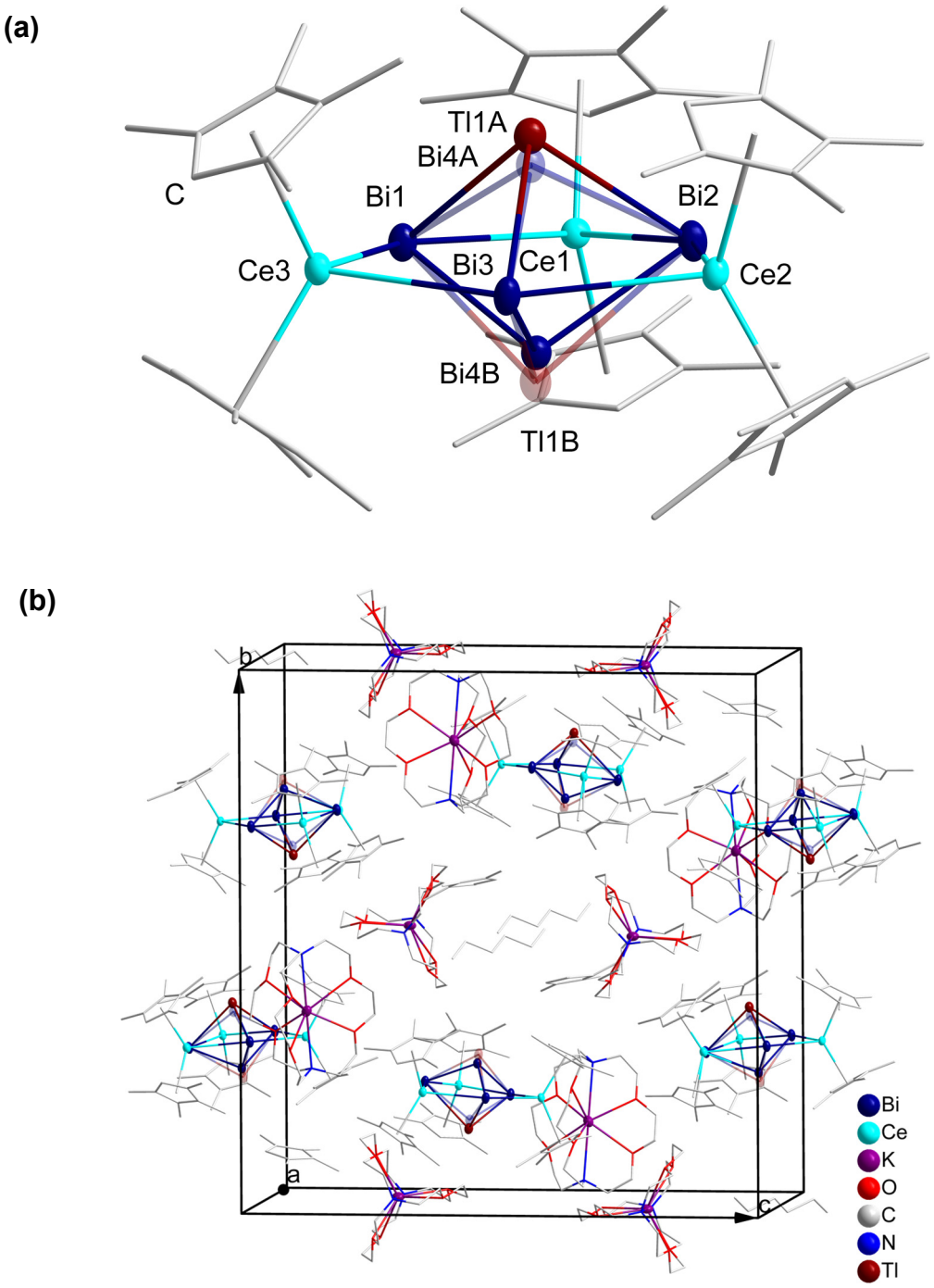

Supplementary Figure 3 | Crystal structure of [K(crypt-222)]$_2$[2]·0.25($C_5Me_4H_2$)·0.25*n*-hexane. a, Side view of the anion $[\mathbf{2}]^{2-}$ with atom labelling scheme of the heavy atoms and illustration of the 50:50 statistical disorder of the Tl1 and Bi4 atoms. **b,** View of the unit cell of [K(crypt-222)]$_2$[**2**]·0.25($C_5Me_4H_2$)·0.25*n*-hexane. H atoms are omitted for clarity. All non-hydrogen atoms except for those of the free $C_5Me_4H_2$ and *n*-hexane molecules were refined using anisotropic displacement parameters. All hydrogen atoms were refined by using a riding model.

4. X-ray Fluorescence Spectroscopy (μ-XFS)

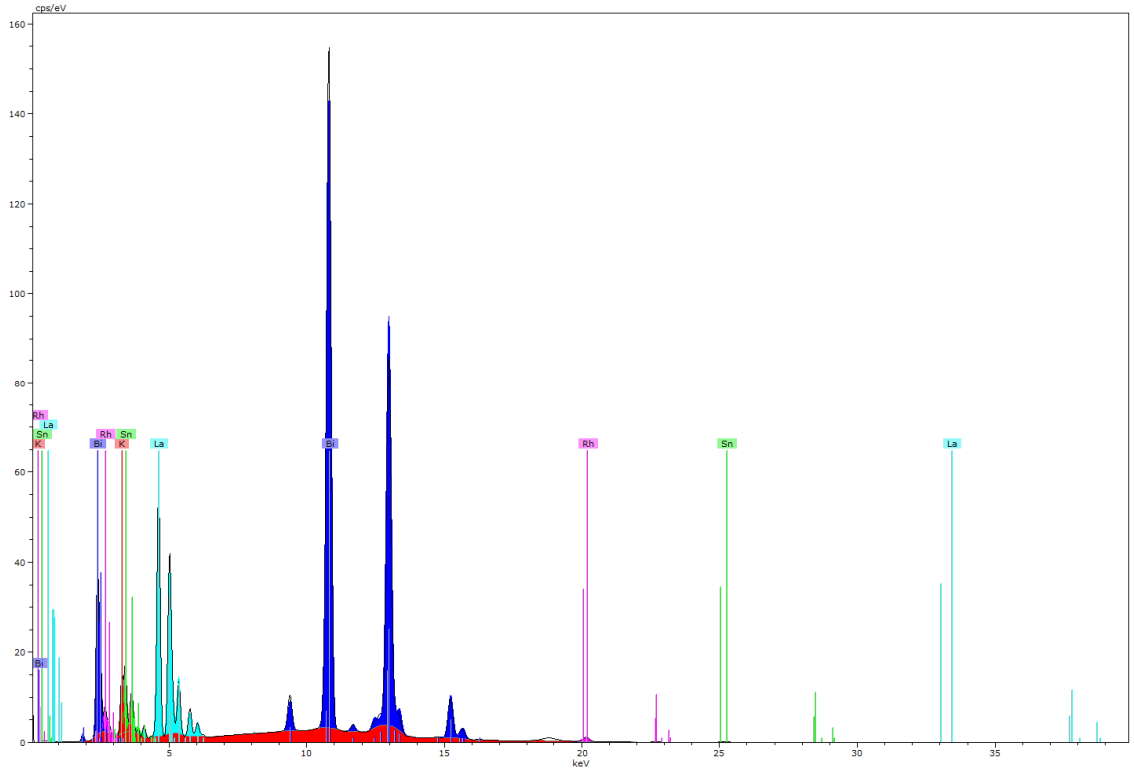

Supplementary Figure 4 | μ-XFS spectrum of compound [K(crypt-222)]$_2$[1]·0.66(C_6H_5Me). Colors are used as follows: K (orange), La (turquoise), Sn (green), Bi (blue).

Supplementary Table 3 | Results of the μ-XFS measurement of compound [K(crypt-222)]$_2$[1]·0.66(C_6H_5Me).

Element	Atomic No.	Netto	Mass [%]	Atom Cont. Obs. [%]	Atom Cont. Calc. [%]
La	57	3216232	28.6	37.3 ≙ 3.0 atoms (of 8)	37.5 ≙ 3 atoms (of 8)
Sn	50	581490	15.0	20.9 ≙ 1.7 atoms (of 8)	25.0 ≙ 2 atoms (of 8)
Bi	83	9997648	48.5	42.0 ≙ 3.3 atoms (of 8)	37.5 ≙ 3 atoms (of 8)

Within the error of the method, the numbers agree very well with the calculated values.

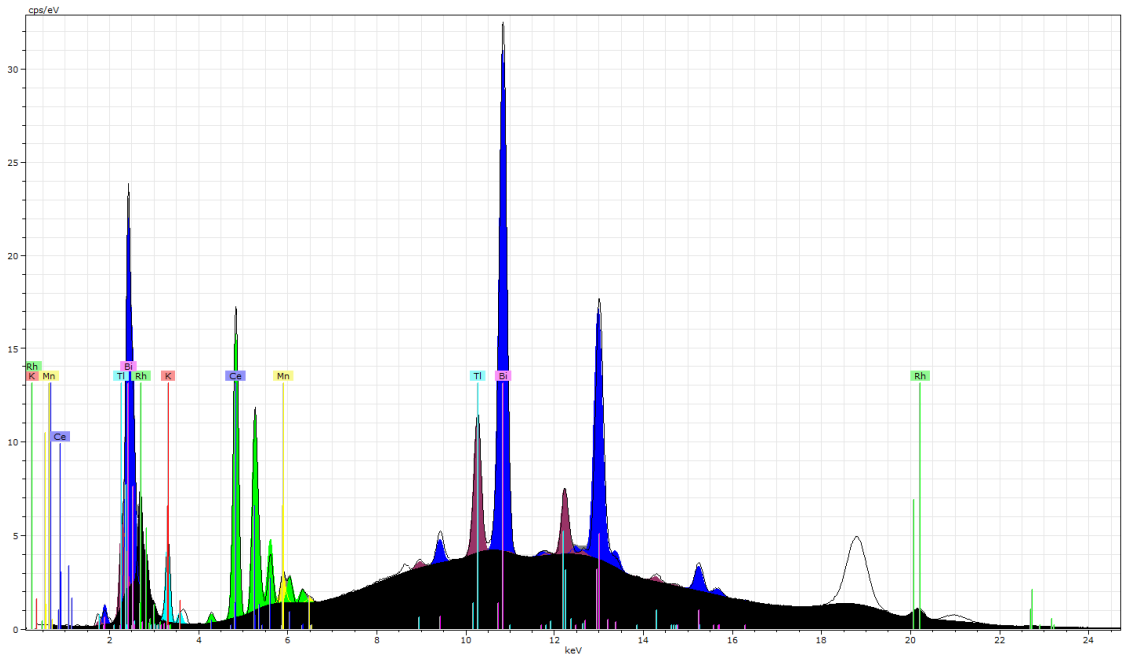

Supplementary Figure 5 | *μ*-XFS spectrum of compound [K(crypt-222)]$_2$[2]·0.25($C_5Me_4H_2$)·0.25*n*-hexane. Colors are used as follows: K (turquoise), Ce (green), Tl (brown), Bi (blue).

Supplementary Table 4 | Results of the *μ*-XFS measurement of compound [K(crypt-222)]$_2$[2]·0.25($C_5Me_4H_2$)·0.25*n*-hexane.

Element	Atomic No.	Netto	Mass [%]	Atom Cont. Obs. [%]	Atom Cont. Calc. [%]
Ce	58	872115	30.51	45.0 ≙ 3.6 atoms (of 8)	30 ≙ 3 atoms (of 8)
Tl	81	432726	10.40	10.8 ≙ 0.9 atoms (of 8)	10 ≙ 1 atom (of 8)
Bi	83	1719136	43.72	44.2 ≙ 3.5 atoms (of 8)	40 ≙ 4 atoms (of 8)

Within the error of the method, the numbers agree rather well with the calculated values. The fact that the Ce content is slightly overestimated while the Tl and Bi content is slightly underestimated can be ascribed to the relatively high background that affects the accuracy of the measurement especially in the heaviest atom regions.

5. ^{1}H NMR Spectroscopy

^{1}H NMR spectrum of the reactant [La(C$_5$Me$_4$H)$_3$] in solution

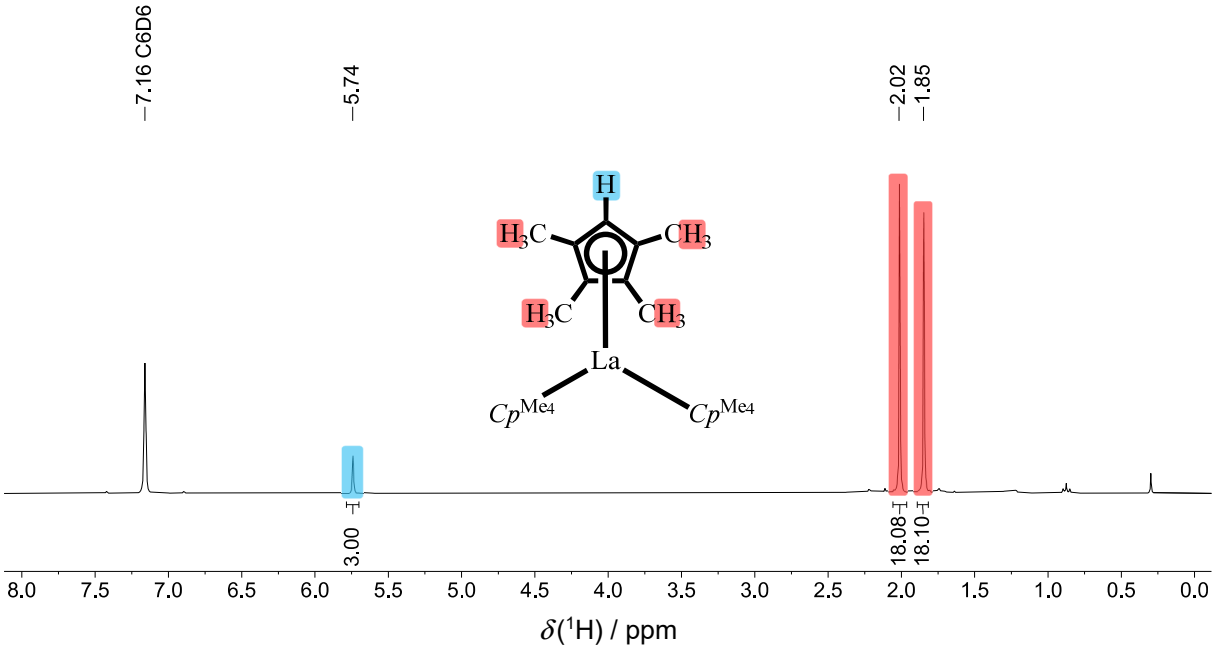

Supplementary Figure 6 | ^{1}H NMR spectrum (300 MHz, C$_6$D$_6$, 298 K) of the reactant [La(C$_5$Me$_4$H)$_3$]. (C$_5$Me$_4$H)$^-$ ligands are denoted as *Cp*^{Me4}. For clarity, a color code is used for the assignment of the signals to the respective hydrogen atoms.

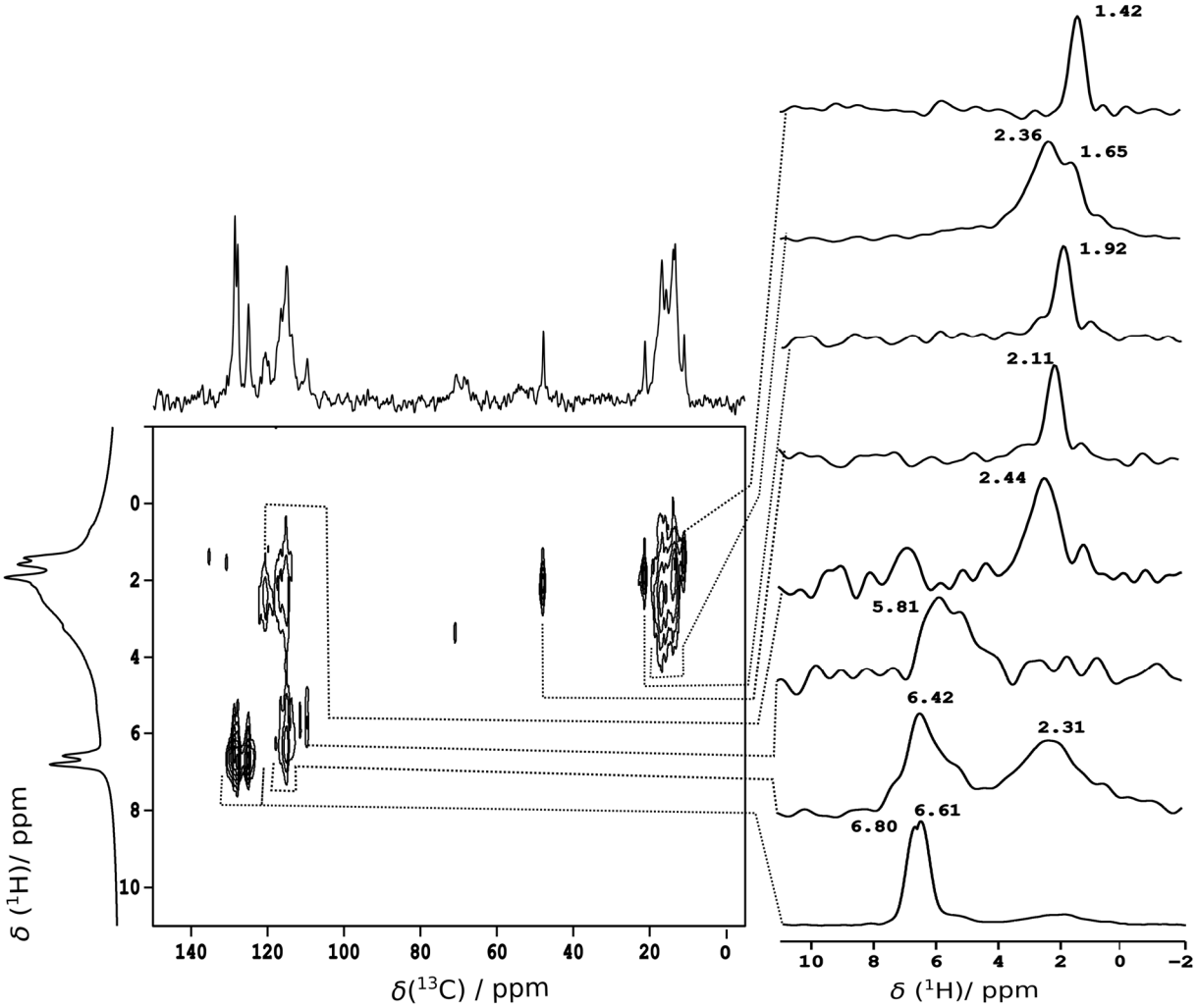

Supplementary Figure 7 | 2D ^{13}C-^{1}H heteronuclear correlation spectrum of [K(crypt-222)]$_2$[1]·0.66(C_6H_5Me) using heteronuclear 2D CP-MAS at a spinning frequency of 20 kHz. The top spectrum is a separate 1D ^{13}C MAS NMR spectrum extracted by sum projection. The left one corresponds to separate 1D ^{1}H MAS NMR spectrum using the background compensated pulse sequence (DEPTH). The right spectrum corresponds to the ^{1}H sum projections from −5 to 11 ppm, the chemical shift values of the correlation peaks are shown in the figure.

6. Supplementary Details on Quantum Chemical Investigations

Current Density Plot of $[1]^{2-}$

The vector magnitude of the magnetically induced current density calculated in the Bi_3La_3 plane is displayed in **Figure 4a** of the main document. The ring current is evident by the yellowish and greenish contour along the Bi_3La_3 ring. As usual,[1,2] the Bi atoms sustain a local ring current. Such a local ring current does not contribute to the global net ring current. The diatropic current flow is illustrated in **Supplementary Figure 8**. This confirms the global ring current and also shows the local ring currents at the La-organyl fragments.

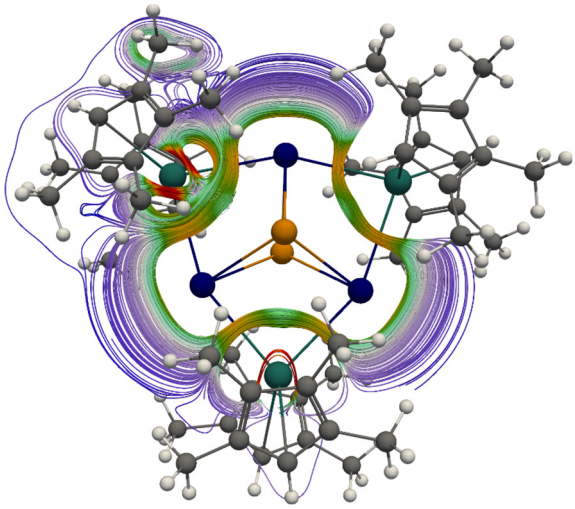

Supplementary Figure 8 | Streamline representation of global and local diatropic ring currents of $[1]^{2-}$. Streamline representation focusing on the local ring current of one La-organyl fragment.

Current Profiles Including Sn Contributions of $[1]^{2-}$

To quantify the ring current flow, a numerical integration is performed. Here, an integration plane is placed through a bond or an atom. The integration plane starting at the global zero point of the magnetically induced ring current (see **Fig. 4** in the main document) is shown in **Supplementary Figure 9**. This integration plane can be cut into small slices of a width Δ to obtain a so-called current profile with respect to the distance or the height.[3] For the current profile with respect to the distance (**Supplementary Fig. 10a**), the full plane is cut into slices vertically. For the respective current height profile (**Supplementary Fig. 10b**), the upper or lower half of the integration plane is cut into small slices horizontally.

According to **Supplementary Figure 10a**, there is a strong contribution of the Sn atoms. As the integration plane starts at the center of the Sn atoms, the local ring current is not canceled out similar to Cu_4Li_2.[4] The local ring current of the Bi atom is overlapped by a diatropic current flow outside the cluster, which is indicated by the difference of the two peaks around 4 and 6 bohr. According to **Supplementary Figure 10b** this current flow is directly in the Bi_3La_3 plane. The global maximum of the height profile is due to the local ring current of the Sn atoms. The location of this maximum is in line with the molecular structure and the coordinates of the Sn atoms.

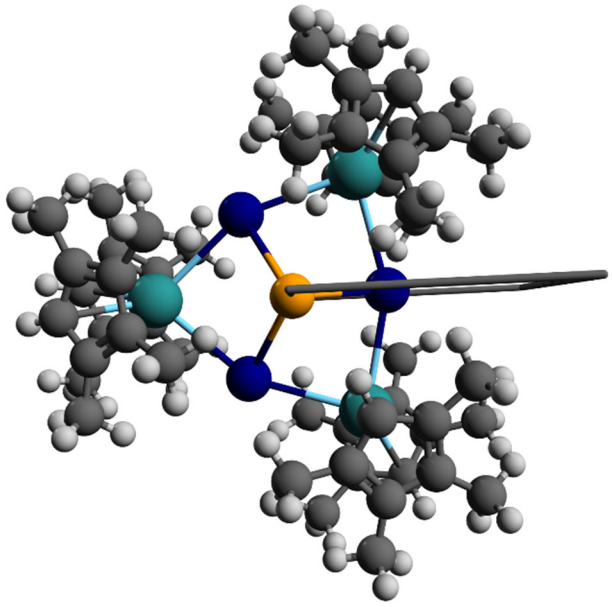

Supplementary Figure 9 | Placement of the integration plane for the current strength calculations including contributions of the Sn atoms of $[1]^{2-}$. Top-view is shown. The magnetic field is perpendicular to the Bi_3La_3 plane.

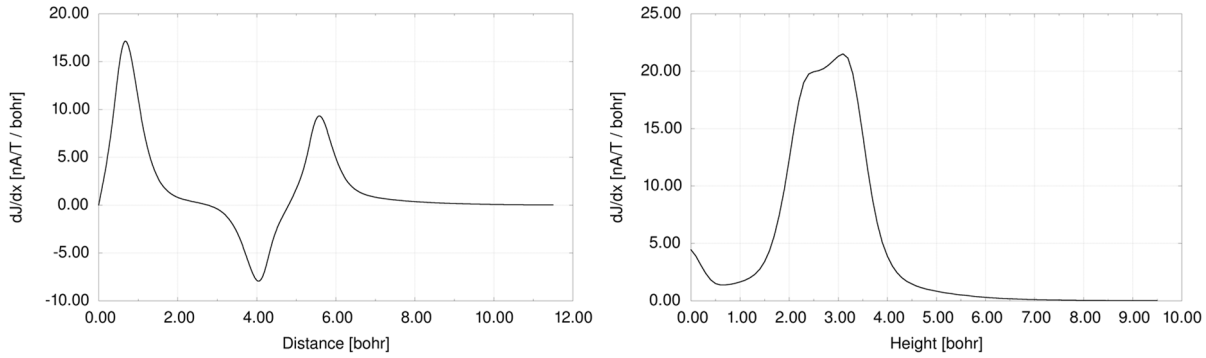

Supplementary Figure 10 | Current density profiles including Sn Contributions of $[1]^{2-}$. **a,** Current density profiles with respect to the distance of the ring current strength. The integration plane ranges from 10 Bohr below to 10 Bohr above the Bi_3La_3 plane. **b,** Current density profiles with respect to the height of the ring current strength. The integration plane ranges about 10 Bohr outside the cluster to ensure convergence with respect to the distance (see a); the profiles start at the global zero point of the magnetically induced current density. A positive sign indicates a diatropic contribution. The sharp peaks (1 bohr distance and 3 bohr height) are due to the local ring currents of the Sn atoms. According to the current height profile, there is a current flow in the Bi_3La_3 plane.

Current Profiles Excluding Sn Contributions

To study the current flow through the Bi_3La_3 ring itself, we shrink the integration plane as shown in **Supplementary Figure 11**, i.e., we reduce the distance for the integration inside the cluster. The plane still ranges from 10 Bohr below to 10 Bohr above the Bi_3La_3 plane. The respective current profiles are displayed in **Supplementary Figure 12**. Here, the width and height of the second peak, i.e. that of the spatial region outside the cluster, is increased, and the height profile shows a sharp peak in the Bi_3La_3 plane. A weak diatropic current flow ranges from 1 to 5 bohr above the Bi_3La_3 plane.

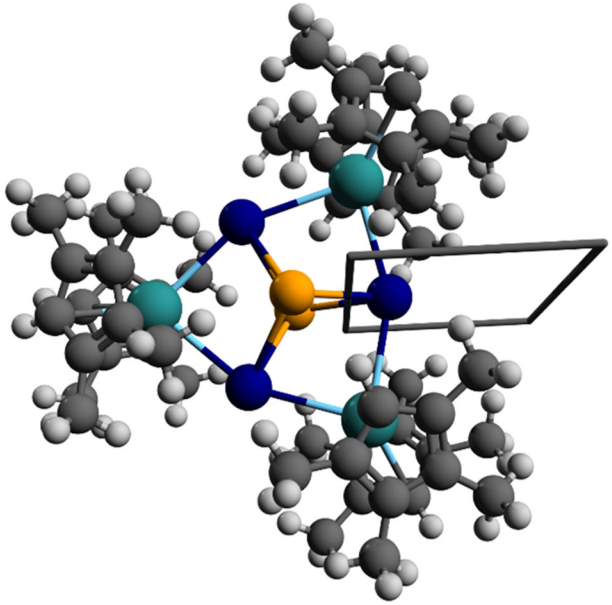

Supplementary Figure 11 | Placement of the integration plane for the current strength calculations excluding contributions of the Sn atoms of $[1]^{2-}$. Top-view is shown. The magnetic field is perpendicular to the Bi_3La_3 plane.

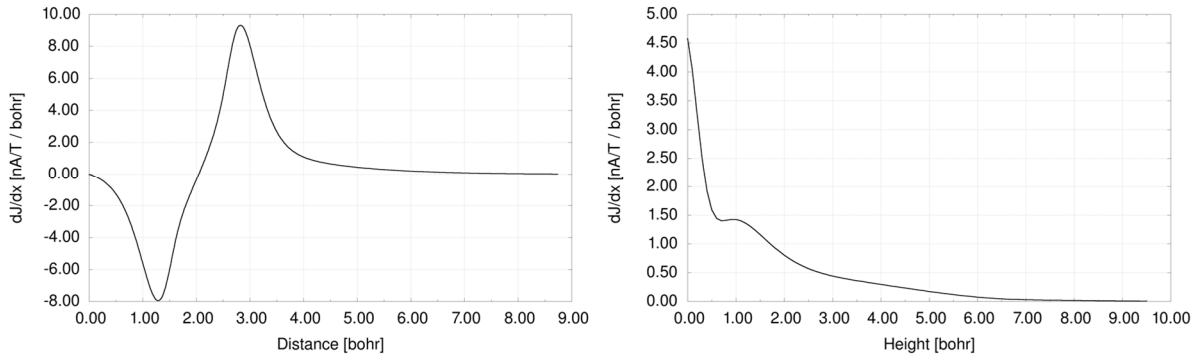

Supplementary Figure 12 | Current density profiles excluding Sn Contributions of $[1]^{2-}$. a, Current density profiles with respect to the distance of the ring current strength. **b,** Current density profiles with respect to the height of the ring current strength. The profiles start at the zero point of the magnetically induced current density beneath the Bi atom. A positive sign indicates a diatropic contribution. The current distance profile shows a net diatropic current flow outside the cluster and the current height profile shows a current flow in the Bi_3La_3 plane.

Current strengths and NICS of $[1]^{2-}$

The current strengths and NICS values of $[\mathbf{1}]^{2-}$ are listed in **Supplementary Table 5** for the integration plane in **Supplementary Figure 11**, i.e., for the integration plane without the local Sn contributions. The (isotropic) NICS value at the center of mass of about −17 nA/T is mainly caused by the contribution of the SCF density, which amounts to −53 ppm. In contrast, the CPKS density contribution is +36 ppm. In detail, the paramagnetic unperturbed and perturbed density term (see Ref. 5,6) cancel each other almost completely. Note that the NICS tensor shows large contributions for the zz element (−46.3 ppm), while all other elements are comparably small and almost vanish (1–3 ppm in absolute numbers). Due to the similar results with the ECP-based Hamiltonian and the all-electron Hamiltonian, the valence electrons are responsible for this NICS tensor and value.

The current strength calculations confirm the observations of the current profiles, i.e., a net diatropic ring current strength of about +14 nA/T is obtained. Restricting the integration plane to 0.5 bohr above and below the Bi_3La_3 plane yields a ring current of +5 nA/T. Therefore, a considerably current flow directly in the Bi_3La_3 plane is evident similar to the σ-aromatic Cu_4Li_2,[1,4] for which we obtain +2.1 nA/T in the region of 0.5 bohr above and below the Cu_4 plane. The total ring current strength of Cu_4Li_2 amounts to +18.2 nA/T with the respective computational settings.

The findings of the NICS tensor is confirmed by a current strength calculation with a plane for the magnetic field along the x axes as shown in **Supplementary Figure 13**. Such a placement considers the potential ring current of the Sn_2Bi_2 fragment. This leads to a substantially decreased current strength of only +2.9 to +4.5 nA/T calculated with the TPSS density functional approximation. Therefore, the compound predominately features a σ-type ring current.

Supplementary Table 5 | Current strengths in nA/T and NICS values of $[1]^{2-}$ in ppm. The ghost atom for NICS is placed at the center of mass. DLU-X2C calculations could not be converged regarding the number of grid points for the numerical integration. cTPSS indicates that the paramagnetic current density is used to generalize the kinetic-energy density. TPSS employs the vector potential of the external magnetic field. Here, we only list the results with the default settings for COSMO (epsilon = infinity). For NICS and ring currents with all functionals and COSMO(DMF) settings, see the spreadsheet NICS_and_Currents.xlsx of the zip archive NMR-Calculations.zip.

Functional	ECP/def2-TZVP		DLU-X2C/x2c-TZVPall-s	
	Ring Current	NICS	Ring Current	NICS
TPSS	+14.1	−17.0	–	−15.7
cTPSS	+14.2	−17.2	–	−15.9
cTPSSh	+14.3	–17.2	–	–15.9
PBE0	+14.3	–16.5	–	–15.2
ωB97X-D	+14.5	–16.0	–	–14.6
cTMHF	+15.0	–17.5	–	–16.3

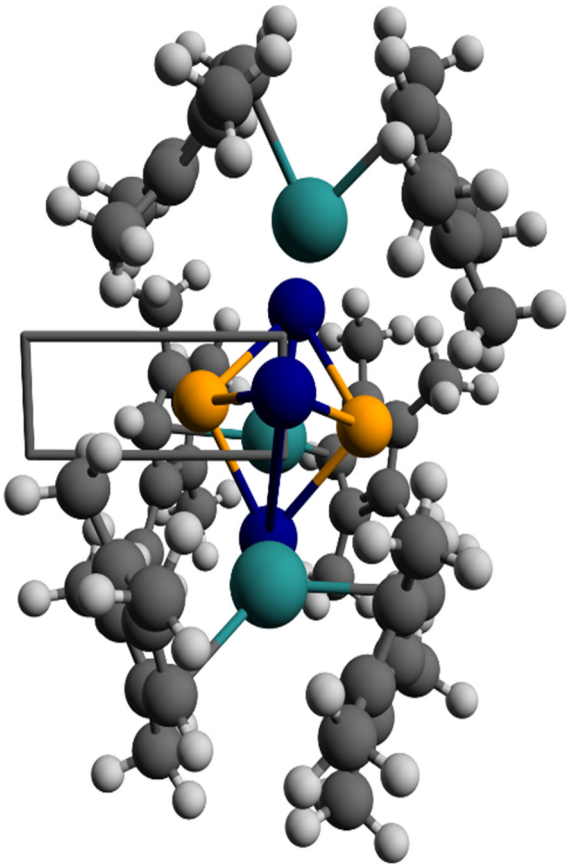

Supplementary Figure 13 | Placement of the integration plane for the current strength calculations of the Sn_2Bi_2 fragment of $[1]^{2-}$. The magnetic field is perpendicular to the Sn-Sn connection line and parallel to the integration plane. Bi–La connection lines are omitted to show the integration plane.

Calculated ^{1}H NMR Shifts of $[1]^{2-}$

The calculated ^{1}H NMR Shifts of $[\mathbf{1}]^{2-}$ with the TPSS, cTPSS, cTPSSh, PBE0, ωB97X-D, and cTMHF density functional approximations are listed in **Supplementary Tables 6–11**. Including spin-orbit effects by extending the scalar X2C framework to the two-component generalization did not notably change the results, i.e., the average shifts are 6.03, 2.06, and 2.34 ppm (spin-orbit) vs. 5.97, 2.16, and 2.27 ppm (scalar) with TPSS. Similar findings hold for PBE0 and ωB97X-D. Here, the shifts change by less than 0.1 ppm upon the inclusion of spin-orbit coupling.

Supplementary Table 6 | Summary of calculated NMR shifts of $[1]^{2-}$ in ppm with TPSS. Calculated values are given for two conditions, under consideration of the respective solvent and under consideration of a conductor-like continuum (ε = ∞). The positions of the H atoms of the Me groups are given with respect to their position on the C_5 ring, and those of the H atoms of the C–H groups (grey background) are given relative to the Sn/Bi cluster core (towards or outwards) are listed. For all shieldings and shifts, see the spreadsheets 1H-LaSnBi_ECP.xlsx and 1H-LaSnBi_X2C.xlsx of the zip archive NMR-Calculations.zip.

		ECP/def2-TZVP		DLU-X2C/x2c-TZVPall-s	
		DMF	ε = ∞	DMF	ε = ∞
$C_5Me_4\boldsymbol{H}$	5 (H "in")	6.68	6.52	6.80	6.55
$C_5Me_4\boldsymbol{H}$	5 (H "out")	5.28	5.14	5.39	5.23
$C_5Me_4\boldsymbol{H}$	average	5.75	5.60	5.86	5.70
$C_5\boldsymbol{Me_4}H$	1, 4 (average)	1.95	1.81	2.04	1.89
	2, 3 (average)	2.10	1.95	2.16	2.00

Supplementary Table 7 | Summary of calculated NMR shifts of $[1]^{2-}$ in ppm with cTPSS. Calculated values are given for two conditions, under consideration of the respective solvent and under consideration of a conductor-like continuum (ε = ∞). The positions of the H atoms of the Me groups are given with respect to their position on the C_5 ring, and those of the H atoms of the C–H groups (grey background) are given relative to the Sn/Bi cluster core (towards or outwards) are listed. For all shieldings and shifts, see the spreadsheets 1H-LaSnBi_ECP.xlsx and 1H-LaSnBi_X2C.xlsx of the zip archive NMR-Calculations.zip.

		ECP/def2-TZVP		DLU-X2C/x2c-TZVPall-s	
		DMF	ε = ∞	DMF	ε = ∞
$C_5Me_4\boldsymbol{H}$	5 (H "in")	6.70	6.53	6.81	6.64
$C_5Me_4\boldsymbol{H}$	5 (H "out")	5.29	5.15	5.36	5.22
$C_5Me_4\boldsymbol{H}$	average	5.76	5.61	5.84	5.69
$C_5\boldsymbol{Me_4}H$	1, 4 (average)	1.96	1.81	2.03	1.88
	2, 3 (average)	2.11	1.96	2.15	1.99

Supplementary Table 8 | Summary of calculated NMR shifts of $[1]^{2-}$ in ppm with cTPSSh. Calculated values are given for two conditions, under consideration of the respective solvent and under consideration of a conductor-like continuum (ε = ∞). The positions of the H atoms of the Me groups are given with respect to their position on the C_5 ring, and those of the H atoms of the C–H groups (grey background) are given relative to the Sn/Bi cluster core (towards or outwards) are listed. For all shieldings and shifts, see the spreadsheets 1H-LaSnBi_ECP.xlsx and 1H-LaSnBi_X2C.xlsx of the zip archive NMR-Calculations.zip.

		ECP/def2-TZVP		DLU-X2C/x2c-TZVPall-s	
		DMF	ε = ∞	DMF	ε = ∞
$C_5Me_4\boldsymbol{H}$	5 (H "in")	6.60	6.43	6.72	6.55
$C_5Me_4\boldsymbol{H}$	5 (H "out")	5.27	5.13	5.35	5.21
$C_5Me_4\boldsymbol{H}$	average	5.71	5.56	5.80	5.65
$C_5\boldsymbol{Me_4}H$	1, 4 (average)	1.89	1.74	1.97	1.81
	2, 3 (average)	2.04	1.89	2.08	1.92

Supplementary Table 9 | Summary of calculated NMR shifts of $[1]^{2-}$ in ppm with PBE0. Calculated values are given for two conditions, under consideration of the respective solvent and under consideration of a conductor-like continuum (ε = ∞). The positions of the H atoms of the Me groups are given with respect to their position on the C_5 ring, and those of the H atoms of the C–H groups (grey background) are given relative to the Sn/Bi cluster core (towards or outwards) are listed. For all shieldings and shifts, see the spreadsheets 1H-LaSnBi_ECP.xlsx and 1H-LaSnBi_X2C.xlsx of the zip archive NMR-Calculations.zip.

		ECP/def2-TZVP		DLU-X2C/x2c-TZVPall-s	
		DMF	ε = ∞	DMF	ε = ∞
$C_5Me_4\boldsymbol{H}$	5 (H "in")	6.49	6.31	6.58	6.39
$C_5Me_4\boldsymbol{H}$	5 (H "out")	5.19	5.04	5.26	5.10
$C_5Me_4\boldsymbol{H}$	average	5.62	5.46	5.69	5.63
$C_5\boldsymbol{Me_4}H$	1, 4 (average)	1.74	1.58	1.79	1.63
	2, 3 (average)	1.89	1.73	1.90	1.74

Supplementary Table 10 | Summary of calculated NMR shifts of $[1]^{2-}$ in ppm with ωB97X-D. Calculated values are given for two conditions, under consideration of the respective solvent and under consideration of a conductor-like continuum (ε = ∞). The positions of the H atoms of the Me groups are given with respect to their position on the C_5 ring, and those of the H atoms of the C–H groups (grey background) are given relative to the Sn/Bi cluster core (towards or outwards) are listed. For all shieldings and shifts, see the spreadsheets 1H-LaSnBi_ECP.xlsx and 1H-LaSnBi_X2C.xlsx of the zip archive NMR-Calculations.zip.

		ECP/def2-TZVP		DLU-X2C/x2c-TZVPall-s	
		DMF	ε = ∞	DMF	ε = ∞
C_5Me_4***H***	5 (H "in")	6.28	6.08	6.35	6.16
C_5Me_4***H***	5 (H "out")	5.25	5.09	5.30	5.14
C_5Me_4***H***	average	5.59	5.43	5.65	5.48
C_5***Me*$_4$**H	1, 4 (average)	1.70	1.54	1.73	1.56
	2, 3 (average)	1.84	1.67	1.83	1.66

Supplementary Table 11 | Summary of calculated NMR shifts of $[1]^{2-}$ in ppm with cTMHF. Calculated values are given for two conditions, under consideration of the respective solvent and under consideration of a conductor-like continuum (ε = ∞). The positions of the H atoms of the Me groups are given with respect to their position on the C_5 ring, and those of the H atoms of the C–H groups (grey background) are given relative to the Sn/Bi cluster core (towards or outwards) are listed. For all shieldings and shifts, see the spreadsheets 1H-LaSnBi_ECP.xlsx and 1H-LaSnBi_X2C.xlsx of the zip archive NMR-Calculations.zip.

		ECP/def2-TZVP		DLU-X2C/x2c-TZVPall-s	
		DMF	ε = ∞	DMF	ε = ∞
C_5Me_4***H***	5 (H "in")	6.48	6.30	6.38	6.20
C_5Me_4***H***	5 (H "out")	5.36	5.22	5.23	5.09
C_5Me_4***H***	average	5.73	5.58	5.62	5.46
C_5***Me*$_4$**H	1, 4 (average)	1.68	1.53	1.56	1.40
	2, 3 (average)	1.81	1.66	1.65	1.49

Calculated ^{1}H NMR Shifts of the Reactant [La($C_5Me_4H)_3$]

The calculated ^{1}H NMR Shifts of a hypothetical complex "[La($C_5Me_4H)_2$]Br" with the TPSS, cTPSS, cTPSSh, PBE0, ωB97X-D, and cTMHF density functional approximations are listed in **Supplementary Tables 12–17**.

Supplementary Table 12 | Summary of calculated NMR shifts of the reactant [La($C_5Me_4H)_3$] in ppm with TPSS. Calculated values are given for two conditions, under consideration of the respective solvent and under consideration of a conductor-like continuum (ε = ∞). The positions of the H atoms of the Me groups are given with respect to their position on the C_5 ring. For all shieldings and shifts, see the spreadsheets 1H-LaCp3-Reactant_ECP.xlsx and 1H-LaCp3-Reactant_X2C.xlsx of the zip archive NMR-Calculations.zip.

		ECP/def2-TZVP		DLU-X2C/x2c-TZVPall-s	
		Benzene	ε = ∞	Benzene	ε = ∞
C_5Me_4***H***	5 (average)	5.46	5.27	5.48	5.36
C_5***Me***$_4$H	1, 4 (average)	1.41	1.29	1.46	1.35
	2, 3 (average)	1.60	1.48	1.63	1.50

Supplementary Table 13 | Summary of calculated NMR shifts of the reactant [La($C_5Me_4H)_3$] in ppm with cTPSS. Calculated values are given for two conditions, under consideration of the respective solvent and under consideration of a conductor-like continuum (ε = ∞). The positions of the H atoms of the Me groups are given with respect to their position on the C_5 ring. For all shieldings and shifts, see the spreadsheets 1H-LaCp3-Reactant_ECP.xlsx and 1H-LaCp3-Reactant_X2C.xlsx of the zip archive NMR-Calculations.zip.

		ECP/def2-TZVP		DLU-X2C/x2c-TZVPall-s	
		Benzene	ε = ∞	Benzene	ε = ∞
C_5Me_4***H***	5 (average)	5.46	5.33	5.47	5.34
C_5***Me***$_4$H	1, 4 (average)	1.40	1.29	1.45	1.34
	2, 3 (average)	1.60	1.48	1.62	1.50

Supplementary Table 14 | Summary of calculated NMR shifts of the reactant [La($C_5Me_4H)_3$] in ppm with cTPSSh. Calculated values are given for two conditions, under consideration of the respective solvent and under consideration of a conductor-like continuum (ε = ∞). The positions of the H atoms of the Me groups are given with respect to their position on the C_5 ring. For all shieldings and shifts, see the spreadsheets 1H-LaCp3-Reactant_ECP.xlsx and 1H-LaCp3-Reactant_X2C.xlsx of the zip archive NMR-Calculations.zip.

		ECP/def2-TZVP		DLU-X2C/x2c-TZVPall-s	
		Benzene	ε = ∞	Benzene	ε = ∞
C_5Me_4***H***	5 (average)	5.43	5.30	5.44	5.31
C_5***Me***$_4$H	1, 4 (average)	1.35	1.24	1.40	1.28
	2, 3 (average)	1.55	1.42	1.56	1.44

Supplementary Table 15 | Summary of calculated NMR shifts of the reactant [La($C_5Me_4H)_3$] in ppm with PBE0. Calculated values are given for two conditions, under consideration of the respective solvent and under consideration of a conductor-like continuum (ε = ∞). The positions of the H atoms of the Me groups are given with respect to their position on the C_5 ring. For all shieldings and shifts, see the spreadsheets 1H-LaCp3-Reactant_ECP.xlsx and 1H-LaCp3-Reactant_X2C.xlsx of the zip archive NMR-Calculations.zip.

		ECP/def2-TZVP		DLU-X2C/x2c-TZVPall-s	
		Benzene	ε = ∞	Benzene	ε = ∞
C_5Me_4***H***	5 (average)	5.32	5.19	5.33	5.20
C_5***Me***$_4$H	1, 4 (average)	1.19	1.08	1.21	1.09
	2, 3 (average)	1.38	1.25	1.38	1.25

Supplementary Table 16 | Summary of calculated NMR shifts of the reactant [La($C_5Me_4H)_3$] in ppm with ωB97X-D. Calculated values are given for two conditions, under consideration of the respective solvent and under consideration of a conductor-like continuum (ε = ∞). The positions of the H atoms of the Me groups are given with respect to their position on the C_5 ring. For all shieldings and shifts, see the spreadsheets 1H-LaCp3-Reactant_ECP.xlsx and 1H-LaCp3-Reactant_X2C.xlsx of the zip archive NMR-Calculations.zip.

		ECP/def2-TZVP		DLU-X2C/x2c-TZVPall-s	
		Benzene	ε = ∞	Benzene	ε = ∞
C_5Me_4***H***	5 (average)	5.35	5.22	5.37	5.23
C_5***Me***$_4$H	1, 4 (average)	1.16	1.05	1.18	1.06
	2, 3 (average)	1.36	1.23	1.35	1.22

Supplementary Table 17 | Summary of calculated NMR shifts of the reactant [La($C_5Me_4H)_3$] in ppm with cTMHF. Calculated values are given for two conditions, under consideration of the respective solvent and under consideration of a conductor-like continuum (ε = ∞). The positions of the H atoms of the Me groups are given with respect to their position on the C_5 ring. For all shieldings and shifts, see the spreadsheets 1H-LaCp3-Reactant_ECP.xlsx and 1H-LaCp3-Reactant_X2C.xlsx of the zip archive NMR-Calculations.zip.

		ECP/def2-TZVP		DLU-X2C/x2c-TZVPall-s	
		Benzene	ε = ∞	Benzene	ε = ∞
C_5Me_4***H***	5 (average)	5.32	5.18	5.33	5.19
C_5***Me***$_4$H	1, 4 (average)	0.97	0.86	0.98	0.86
	2, 3 (average)	1.16	1.04	1.14	1.02

Calculated ^{1}H NMR Shifts of a Hypothetical Complex "[La($C_5Me_4H)_2$]Br"

The calculated ^{1}H NMR Shifts of a hypothetical complex "[La($C_5Me_4H)_2$]Br" with the TPSS, cTPSS, cTPSSh, PBE0, ωB97X-D, and cTMHF density functional approximations are listed in **Supplementary Tables 18–23**.

Supplementary Table 18 | Summary of calculated NMR shifts of a hypothetical complex "[La($C_5Me_4H)_2$]Br" in ppm with TPSS. Calculated values are given for two conditions, under consideration of the respective solvent and under consideration of a conductor-like continuum (ε = ∞). The positions of the H atoms of the Me groups are given with respect to their position on the C_5 ring, and those of the H atoms of the C–H groups (grey background) are given relative to the Sn/Bi cluster core (towards or outwards) are listed. For all shieldings and shifts, see the spreadsheets 1H-Hypothetical-Mononuc-Br_ECP.xlsx and 1H-Hypothetical-Mononuc-Br_X2C.xlsx of the zip archive NMR-Calculations.zip.

		ECP/def2-TZVP		DLU-X2C/x2c-TZVPall-s	
		DMF	ε = ∞	DMF	ε = ∞
C_5Me_4***H***	5 (H "in")	5.93	5.77	5.88	5.72
C_5Me_4***H***	5 (H "out")	5.96	5.82	6.02	5.88
C_5***Me*****$_4$**H	1, 4 (average)	1.90	1.64	1.84	1.69
	2, 3 (average)	2.08	1.82	1.99	1.83

Supplementary Table 19 | Summary of calculated NMR shifts of a hypothetical complex "[La($C_5Me_4H)_2$]Br" in ppm with cTPSS. Calculated values are given for two conditions, under consideration of the respective solvent and under consideration of a conductor-like continuum (ε = ∞). The positions of the H atoms of the Me groups are given with respect to their position on the C_5 ring, and those of the H atoms of the C–H groups (grey background) are given relative to the Sn/Bi cluster core (towards or outwards) are listed. For all shieldings and shifts, see the spreadsheets 1H-Hypothetical-Mononuc-Br_ECP.xlsx and 1H-Hypothetical-Mononuc-Br_X2C.xlsx of the zip archive NMR-Calculations.zip.

		ECP/def2-TZVP		DLU-X2C/x2c-TZVPall-s	
		DMF	ε = ∞	DMF	ε = ∞
C_5Me_4***H***	5 (H "in")	5.94	5.78	5.88	5.71
C_5Me_4***H***	5 (H "out")	5.97	5.82	6.02	5.87
C_5***Me*****$_4$**H	1, 4 (average)	1.79	1.64	1.83	1.68
	2, 3 (average)	1.97	1.82	1.98	1.83

Supplementary Table 20 | Summary of calculated NMR shifts of a hypothetical complex "[La($C_5Me_4H)_2$]Br" in ppm with cTPSSh. Calculated values are given for two conditions, under consideration of the respective solvent and under consideration of a conductor-like continuum (ε = ∞). The positions of the H atoms of the Me groups are given with respect to their position on the C_5 ring, and those of the H atoms of the C–H groups (grey background) are given relative to the Sn/Bi cluster core (towards or outwards) are listed. For all shieldings and shifts, see the spreadsheets 1H-Hypothetical-Mononuc-Br_ECP.xlsx and 1H-Hypothetical-Mononuc-Br_X2C.xlsx of the zip archive NMR-Calculations.zip.

		ECP/def2-TZVP		DLU-X2C/x2c-TZVPall-s	
		DMF	ε = ∞	DMF	ε = ∞
C_5Me_4***H***	5 (H "in")	5.90	5.74	5.85	5.68
C_5Me_4***H***	5 (H "out")	5.95	5.80	6.00	5.85
C_5***Me*$_4$**H	1, 4 (average)	1.74	1.59	1.78	1.63
	2, 3 (average)	1.92	1.77	1.93	1.77

Supplementary Table 21 | Summary of calculated NMR shifts of a hypothetical complex "[La($C_5Me_4H)_2$]Br" in ppm with PBE0. Calculated values are given for two conditions, under consideration of the respective solvent and under consideration of a conductor-like continuum (ε = ∞). The positions of the H atoms of the Me groups are given with respect to their position on the C_5 ring, and those of the H atoms of the C–H groups (grey background) are given relative to the Sn/Bi cluster core (towards or outwards) are listed. For all shieldings and shifts, see the spreadsheets 1H-Hypothetical-Mononuc-Br_ECP.xlsx and 1H-Hypothetical-Mononuc-Br_X2C.xlsx of the zip archive NMR-Calculations.zip.

		ECP/def2-TZVP		DLU-X2C/x2c-TZVPall-s	
		DMF	ε = ∞	DMF	ε = ∞
C_5Me_4***H***	5 (H "in")	5.81	5.64	5.75	5.57
C_5Me_4***H***	5 (H "out")	5.85	5.69	5.89	5.73
C_5***Me*$_4$**H	1, 4 (average)	1.59	1.43	1.60	1.44
	2, 3 (average)	1.77	1.60	1.75	1.59

Supplementary Table 22 | Summary of calculated NMR shifts of a hypothetical complex "[La($C_5Me_4H)_2$]Br" in ppm with ωB97X-D. Calculated values are given for two conditions, under consideration of the respective solvent and under consideration of a conductor-like continuum (ε = ∞). The positions of the H atoms of the Me groups are given with respect to their position on the C_5 ring, and those of the H atoms of the C–H groups (grey background) are given relative to the Sn/Bi cluster core (towards or outwards) are listed. For all shieldings and shifts, see the spreadsheets 1H-Hypothetical-Mononuc-Br_ECP.xlsx and 1H-Hypothetical-Mononuc-Br_X2C.xlsx of the zip archive NMR-Calculations.zip.

		ECP/def2-TZVP		DLU-X2C/x2c-TZVPall-s	
		DMF	ε = ∞	DMF	ε = ∞
C_5Me_4***H***	5 (H "in")	5.76	5.59	5.71	5.53
C_5Me_4***H***	5 (H "out")	5.85	5.69	5.90	5.74
C_5***Me*$_4$**H	1, 4 (average)	1.56	1.40	1.57	1.41
	2, 3 (average)	1.73	1.57	1.72	1.55

Supplementary Table 23 | Summary of calculated NMR shifts of a hypothetical complex "[La($C_5Me_4H)_2$]Br" in ppm with cTMHF. Calculated values are given for two conditions, under consideration of the respective solvent and under consideration of a conductor-like continuum (ε = ∞). The positions of the H atoms of the Me groups are given with respect to their position on the C_5 ring, and those of the H atoms of the C–H groups (grey background) are given relative to the Sn/Bi cluster core (towards or outwards) are listed. For all shieldings and shifts, see the spreadsheets 1H-Hypothetical-Mononuc-Br_ECP.xlsx and 1H-Hypothetical-Mononuc-Br_X2C.xlsx of the zip archive NMR-Calculations.zip.

		ECP/def2-TZVP		DLU-X2C/x2c-TZVPall-s	
		DMF	ε = ∞	DMF	ε = ∞
C_5Me_4***H***	5 (H "in")	5.72	5.55	5.66	5.48
C_5Me_4***H***	5 (H "out")	5.78	5.63	5.82	5.66
C_5***Me*$_4$**H	1, 4 (average)	1.37	1.37	1.37	1.21
	2, 3 (average)	1.53	1.21	1.50	1.34

7. References for the Supporting Information

1. Eulenstein, A. R. et al. Substantial π-aromaticity in the anionic heavy-metal cluster $[Th@Bi_{12}]^{4-}$. *Nat. Chem.* **13**, 149–155 (2021).
2. Peerless, B., Schmidt, A., Franzke, Y. J. & Dehnen, S. φ-Aromaticity in prismatic $\{Bi_6\}$-based clusters. *Nat. Chem.* **15**, 347–356 (2023).
3. Sundholm, D., Fliegl, H. & Berger, R. J. Calculations of magnetically induced current densities: theory and applications. *Wiley Interdiscip. Rev.: Comput. Mol. Sci.* **6**, 639–678 (2016).
4. Lin, Y.-C. et al. Experimental and Computational Studies of Alkali-Metal Coingage-Metal Clusters. *J. Phys. Chem. A.* **110**, 4244–4250 (2006).
5. Franzke, Y. J. & Weigend, F. NMR Shielding Tensors and Chemical Shifts in Scalar-Relativistic Local Exact Two-Component Theory. *J. Chem. Theory Comput.* **15**, 1028–1043 (2019).
6. Reiter, K., Mack, F. & Weigend, F. Calculation of Magnetic Shielding Constants with meta-GGA Functionals Employing the Multipole-Accelerated Resolution of the Identity: Implementation and Assessment of Accuracy and Efficiency. *J. Chem. Theory Comput.* **14**, 191–197 (2018).